

Article

Remote Estimation of Leaf and Canopy Water Content in Winter Wheat with Different Vertical Distribution of Water-Related Properties

Shishi Liu ¹, Yi Peng ^{2,*}, Wei Du ^{1,†}, Yuan Le ^{2,†} and Lu Li ^{1,†}

¹ College of Resources and Environment, Huazhong Agricultural University, Wuhan 430070, China; E-Mails: sslu@mail.hzau.edu.cn (S.L.); weidu@webmail.hzau.edu.cn (W.D.); LULULI@web.mail.hzau.edu.cn (L.L.)

² School of Remote Sensing and Information Engineering, Wuhan University, Wuhan 430079, China; E-Mail: leyuan_rs@whu.edu.cn

† These authors contributed equally to this work.

* Author to whom correspondence should be addressed; E-Mail: ypeng@whu.edu.cn.

Academic Editors: Yoshio Inoue and Prasad S. Thenkabail

Received: 30 October 2014 / Accepted: 8 April 2015 / Published: 17 April 2015

Abstract: This study analyzed the vertical distribution of gravimetric water content (GWC), relative water content (RWC), and equivalent water thickness (EWT) in winter wheat during heading and early ripening stages, and evaluated the position of leaf number at which Vegetation Indexes (VIs) can best retrieve canopy water-related properties of winter wheat. Results demonstrated that the vertical distribution of these properties followed a near-bell-shaped curve with the highest values at the intermediate leaf position. GWC of the top three or four leaves during the heading stage and the top two or three leaves during the early ripening stage can represent the GWC of the whole canopy, but the RWC and EWT of the whole canopy should be calculated based on the top four leaves. At leaf level, the analysis demonstrated strong relationships between EWT and VIs for the top leaf layer, but for GWC_D, GWC_F, and RWC, the strongest relationships with VIs were found in the intermediate leaf layers. At canopy level, VIs provided the most accurate estimation of GWC for the top three or four leaves. Water absorption-based VIs could estimate canopy EWT of winter wheat for the top four leaves, but the suitable bands sensitive to water absorptions should be carefully selected for the studied species.

Keywords: vertical distribution; gravimetric water content (GWC); relative water content (RWC); equivalent water thickness (EWT); vegetation indexes

1. Introduction

Estimating vegetation water-related properties is of significance for evaluating vegetation growth and health status [1]. Water-related properties of vegetation include gravimetric water content (GWC), relative water content (RWC), and equivalent water thickness (EWT). GWC is a measure of absolute water content in leaves, determined on fresh and dry leaf mass. RWC is the volume of leaf water expressed as a fraction of the water volume for the leaf at full turgidity. It is probably the most appropriate measure of plant water status in terms of the physiological consequence of cellular water deficit, and thus has been used as an indicator of plant water stress [2]. EWT is expressed as the volume of water content per unit leaf area. Field sampling of vegetation provides the most accurate measurements of water-related properties, but dynamic changes of vegetation water content and time-consuming procedures preclude effective field monitoring at large scales. Remote sensing techniques offer an instantaneous and non-destructive alternative of monitoring vegetation water content at large scales, which is vital for water stress detection, fire risk assessment, and efficient irrigation scheduling.

Reflectance in the near-infrared (NIR) region (750–1300 nm) and shortwave-infrared (SWIR) region (1300–2500 nm) is largely influenced by water and dry matter in the leaves, although it is also affected by leaf structure, canopy structure, and leaf area index (LAI) [3–5]. Strong water absorption bands can be found in the SWIR region, centered on 1450, 1940, and 2500 nm, and weak water absorption bands are located in the NIR region near 970 and 1200 nm. Therefore, the measurement of radiation reflected by leaves and canopy provides the basis of estimating vegetation water content with remote sensing techniques.

Spectral indexes allow estimation of leaf and canopy water content by means of empirical approaches using regression techniques [6–10]. Moisture Stress Index (MSI) was developed and tested for remote sensing of leaf RWC [11,12]. VIs based on reflectance of NIR and SWIR regions, such as Water Index (WI) [13], Normalized Difference Water Index (NDWI) [4], and Normalized Difference Infrared Index (NDII) [14], have been tested to estimate water content for different vegetation types at both leaf level [15–17] and canopy level [9,15,18–20]. Since GWC is determined on dry mass, the ratios of water indices and dry-matter indices were developed in order to estimate GWC [17]. Although VIs with bands in the visible region are developed to estimate chlorophyll content and LAI, investigations have shown that they are indirectly related to leaf water content through correlations with leaf pigments [21,22]. In addition, several recent studies have used advanced spectroscopic approaches to estimate leaf water content, including radiative transfer modeling inversion [23], artificial neural networks [24], continuous wavelet analysis [25], and partial least squares regression [26,27].

However, when light penetrates the canopy, it is attenuated by scattering and absorption per unit distance through the canopy, which is described by the light extinction coefficient in the Lambert-Beer Law [28]. Therefore, the signal received by remote sensors above the canopy may not represent the interaction of incoming radiation with the whole canopy. It is observed that the sensed reflectance in a

grass canopy would change to the point where additional increase of leaf layers did not result in a change of reflectance [29]. Many research simulated the light penetration path using radiative transfer models [30,31], with the assumption of the vertically homogeneous canopy, which is not true in many cases. In addition, since the light extinction coefficient is affected by canopy architecture such as leaf angle and canopy depth, and also depends on spectrum wavelength, it is inappropriate to use it as a constant along the canopy. The vertical distribution of vegetation biophysical and biochemical properties and leaf angle greatly affects the amount of reflected light, and in turn affects the estimation of vegetation properties. Studies have found that a maize canopy has bell-shaped vertical distribution of LAI [32], chlorophyll content [33], leaf nitrogen content and biomass [34]. The study showed that the red-edge Chlorophyll Index ($CI_{red\ edge}$) sensed the chlorophyll content of the upper seven to nine leaf layers in a maize canopy [33].

Although the vertical heterogeneity of both biophysical and biochemical properties has been recognized and highlighted in many studies [35], the remote estimation of vegetation biophysical parameters seldom considers the vertical heterogeneity of canopy due to its complexity. Particularly, for the estimation of vegetation water-related properties, few studies investigate how the vertical distribution of water-related properties affects the estimation of canopy water-related properties using spectra derived from remotely sensed data. The objectives of this paper are to evaluate the vertical distribution of water-related properties within the winter wheat canopy, analyze the impact of vertical profile on the water-related properties at the canopy level, and determine the vertical position where hyperspectral VIs can sense the canopy water-related properties, as well as the most suitable VIs to estimate leaf and canopy water-related properties of winter wheat.

2. Materials and Methods

2.1. Study Area and Field Campaigns

The study area is located in the experimental rain-fed winter wheat field at the Huazhong Agricultural University (Latitude is N 3028'23.16" and Longitude is E11420'47.28"). In the growing season of 2014, winter wheat was sown on October 28 and 29 (DOY 301 and 302) and harvested on May 20 and 21 (DOY 140 and 141).

Table 1. The day of year (DOY) on which field campaigns were conducted in 2014, the number of plants sampled in each field campaign, and the growth stage.

| Dates | DOY | No. Sampled Plants | The Growth Stage |
|----------|-----|--------------------|------------------|
| 3 April | 93 | 6 | Heading |
| 9 April | 99 | 5 | Heading |
| 23 April | 113 | 6 | Heading |
| 29 April | 119 | 11 | Ripening |
| 8 May | 128 | 10 | Ripening |

Wheat plants were sampled weekly or biweekly in the field during the heading and the early ripening stage in 2014. Table 1 shows the dates of field campaigns, the number of plants sampled in each field campaign, and the growth stage. These dates were chosen to evaluate the vertical

distribution of water content along the canopy when wheat has been fully developed with a five-leaf vertical layer. On each sampling date, plants were randomly selected, and leaves were then numerically labeled from the bottom (leaf 1) to the top (leaf 5) of the canopy (Figure 1). In total, 38 plants were sampled and approximately 190 leaves were collected for analysis.

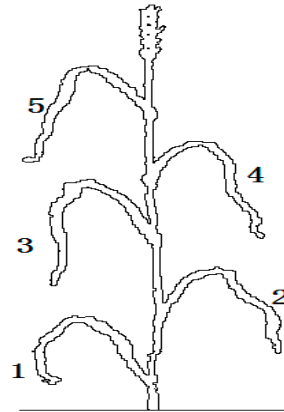


Figure 1. The illustration of the sampled wheat with leaves numerically labeled from the bottom (leaf 1) to the top (leaf 5) of the canopy.

2.2. Reflectance Measurements

For each field campaign, wheat reflectance was measured in the spectral range from 350–2500 nm with a spectral resolution of 1 nm using ASD FieldSpec Pro radiometer at both the leaf and canopy level. The reflectance measurements were conducted on clear days close to solar noon (between 11:00 and 13:00 local time) when changes in solar zenith angle were minimal.

Before measuring canopy reflectance spectra, a spectralon panel (99% reflectance) was scanned to correct variations in the incoming sun illumination. The fiber optic of the ASD radiometer, with an angular field of view of 25°, was placed 0.7 m above the canopy, resulting in a field of view of 0.31 m in diameter at the top of the canopy. The canopy reflectance spectra of the sampled plant were the median of six measurements for each canopy. Leaf reflectance was measured using an ASD radiometer and a self-illuminated leaf probe with a clip attached. On April 23, since the leaf clip did not function well, we did not measure leaf spectra and only measured canopy spectra. When collecting leaf spectra, five random points were selected per leaf, with six spectra scans at each point in the leaf. Thus, a total of 30 spectra were collected per leaf, and their median was used as the leaf reflectance. For each sampled plant, leaf reflectance data was measured at all five leaves from the top to the bottom along the canopy.

Raw leaf and canopy reflectance spectra were then convolved to 5 nm bandwidths for spectral analysis. This bandwidth was selected based on the full width-half maximum of the Airborne Visible/Infrared Imaging Spectrometer (AVIRIS) instrument. For canopy spectra, reflectance between 1320 and 1500 nm, and reflectance between 1730 and 1950 nm were removed, because these water absorption bands are strongly influenced by water vapor in the atmosphere so that they cannot be used for the aircraft- and satellite-based remote sensing.

2.3. Leaf Sampling and Water Content Measurements

After reflectance measurements were taken, all leaves of the sampled plants were cut from the stem with leaf number recorded. They were enclosed in a sealed plastic bag, and brought to the laboratory inside a cooler for leaf area and water content measurements. Fresh weight was recorded using an analytical balance. The area of each leaf was measured five times using a portable leaf area meter YMJ-A (Zhejiang Top Instrument Co., Zhejiang, China) and the median was used for analysis. After measuring leaf area, leaves were immersed in distilled water for 24 h, and weight was recorded as turgid weight. Finally, leaves were dried at 80 °C in an oven, until constant weight (dry weight) was reached.

The gravimetric water content (GWC) of the leaf samples was determined on fresh and dry leaf mass basis as follows:

$$GWC_D = (FM - DM) / DM \quad (1)$$

$$GWC_F = (FM - DM) / FM \quad (2)$$

where GWC_D is the gravimetric water content (grams water/grams dry leaf mass), GWC_F is the gravimetric water content (grams water/grams fresh leaf mass), FM is the fresh leaf mass (g), and DM is the dry leaf mass (g).

The RWC of leaf samples was calculated as:

$$RWC = 100\% \times (FM - DM) / (TM - DM) \quad (3)$$

where TM is turgid weight (g) of the leaf sample.

The EWT of leaf samples was calculated as the volume of water per unit leaf area (cm):

$$EWT = (FM - DM) / (\rho_w \times A) \quad (4)$$

where ρ_w is the density of pure water (1 g/cm³), and A is the leaf area (cm²).

During the ripening stage, the leaves at the bottom two layers of winter wheat were drying down, with minimal water content, thus we removed samples with extremely low water content from the analysis, resulting in 165 samples used in the analysis.

To evaluate the impact of vertical profile on the retrieval of canopy water-related properties using remote sensing VIs, we calculated canopy water-related properties as the value of the top leaf only, the value of the top two leaves, the value of the top three leaves, the value of the top four leaves, and the value of five leaves as follows:

$$Canopy\ GWC_D = \sum_{i=1}^n (FM_i - DM_i) / \sum_{i=1}^n DM_i \quad (5)$$

$$Canopy\ GWC_F = \sum_{i=1}^n (FM_i - DM_i) / \sum_{i=1}^n FM_i \quad (6)$$

$$Canopy\ RWC = \sum_{i=1}^n (FM_i - DM_i) / \sum_{i=1}^n (TM_i - DM_i) \quad (7)$$

$$Canopy\ EWT = \sum_{i=1}^n (FM_i - DM_i) / (\rho_w \times \sum_{i=1}^n A_i) \quad (8)$$

where n is the number of leaves from the top of the canopy, ranging from 1–5. However, since this study lacked the measurements of leaf area index (LAI), EWT calculated with the above equation was the canopy mean value.

2.4. Vegetation Indexes

Leaf and canopy reflectance was used to calculate a wide range of published standard water absorption- and greenness-based VIs, which were previously identified to be good predictors of water content in the literature (Table 2). Note that our calculation of the GVMI did not use rectified NIR reflectance [36,37]. For $CI_{red\ edge}$, ρ_{NIR} is the average reflectance from 750 to 800 nm and $\rho_{red\ edge}$ is the average reflectance from 710 to 730 nm. $(\rho_{850} - \rho_{2218})/(\rho_{850} - \rho_{1928})$ and $(\rho_{850} - \rho_{1788})/(\rho_{850} - \rho_{1928})$ were only evaluated in the leaf-level analysis, not only because they were originally developed based on leaf measurements [8] but also because reflectance at 1788 nm and 1928 nm was noisy in the canopy spectra.

Table 2. Vegetation indexes (VIs) calculated based on leaf and canopy reflectance, including their full names, acronyms, mathematical formulations, and references.

| VI | Formula | References |
|---|---|------------|
| Normalized Difference Vegetation Index (NDVI) | $(\rho_{850} - \rho_{670}) / (\rho_{850} + \rho_{670})$ | [38] |
| Normalized Difference Water Index (NDWI) | $(\rho_{860} - \rho_{1240}) / (\rho_{860} + \rho_{1240})$ | [4] |
| Moisture Stress Index (MSI) | ρ_{1600} / ρ_{819} | [11] |
| Water Index (WI) | ρ_{900} / ρ_{970} | [13] |
| Normalized Difference Infrared Index (NDII) | $(\rho_{819} - \rho_{1600}) / (\rho_{819} + \rho_{1600})$ | [14] |
| Reciprocal of Moisture Stress Index (RMSI) | ρ_{860} / ρ_{1650} | [14] |
| Global Vegetation Moisture Index (GVMI) | $(\rho_{819} + 0.1) - (\rho_{1600} + 0.02) / ((\rho_{819} + 0.1) + (\rho_{1600} + 0.02))$ | [36,37] |
| $(\rho_{850} - \rho_{2218}) / (\rho_{850} - \rho_{1928})$ | $(\rho_{850} - \rho_{2218}) / (\rho_{850} - \rho_{1928})$ | [8] |
| $(\rho_{850} - \rho_{1788}) / (\rho_{850} - \rho_{1928})$ | $(\rho_{850} - \rho_{1788}) / (\rho_{850} - \rho_{1928})$ | [8] |
| Normalized Dry Matter Index (NDMI) | $(\rho_{1649} - \rho_{1722}) / (\rho_{1649} - \rho_{1722})$ | [39] |
| NDII/NDMI | See formulae above | [40] |
| Red-edge Chlorophyll Index ($CI_{red\ edge}$) | $(\rho_{NIR} / \rho_{red\ edge}) - 1$ | [41] |

2.5. Statistics Analysis

Correlation analysis was used to analyze the relationship between reflectance and water-related properties. The least-square linear and non-linear regression techniques were used to build the empirical models between VIs and water-related properties. The statistics used to evaluate the suitability of VIs for estimation of water-related properties included correlation of determination (R^2), p value, and the root mean square error (RMSE). R^2 and p value were used to assess if the variations between measurements and modeled results were significant. The RMSE was used to measure the actual average differences between measurements and modeled results.

3. Results

3.1. The Vertical Distribution of Water-Related Properties of Winter Wheat

GWC, RWC, and EWT are commonly used properties in many studies to indicate vegetation water stress status. The summary statistics for these water-related properties at leaf level are given in Table 3. The ranges of water-related properties of leaves were found to be slightly larger than those reported in some studies [8,9], but within the reasonable range [42].

The correlation between the measured variables is shown in Table 4. It was found that for winter wheat, all these variables were positively correlated with each other, but the correlations of RWC with the other variables were lower than those of the other three variables. The reason for the lower correlation between RWC and the other variables may be that RWC defines water content of wheat in a different way. It was worth noting that GWC was positively correlated with EWT for the wheat leaves studied, which is different to the studies of trees that showed no correlation between GWC and EWT [8,9]. We also ran the correlation analysis between water-related properties for each leaf layer, and results were similar to those shown in Table 4.

Table 3. Summary statistics for water-related properties at leaf level.

| | Mean | Range | Standard Deviation |
|------------------|--------|---------------|--------------------|
| GWC _D | 4.14 | 1.21–7.85 | 1.71 |
| GWC _F | 0.78 | 0.54–0.88 | 0.069 |
| RWC (%) | 76.55% | 46.80%–93.73% | 11.98% |
| EWT (cm) | 0.018 | 0.0067–0.030 | 0.0044 |

Table 4. Correlation coefficients (*r*) among water-related properties at leaf level.

| | GWC _D | GWC _F | RWC (%) | EWT (cm) |
|------------------|------------------|------------------|---------|----------|
| GWC _D | 1 | 0.93 | 0.43 | 0.63 |
| GWC _F | | 1 | 0.42 | 0.68 |
| RWC (%) | | | 1 | 0.38 |
| EWT (cm) | | | | 1 |

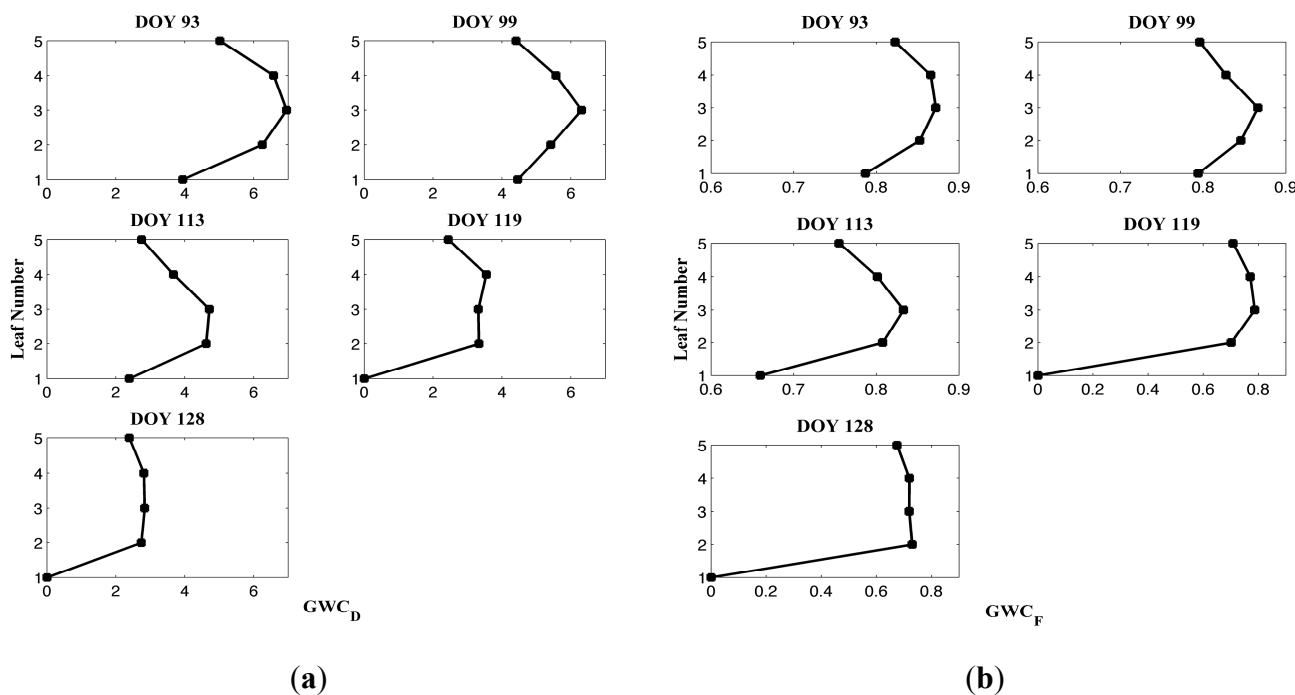


Figure 2. Cont.

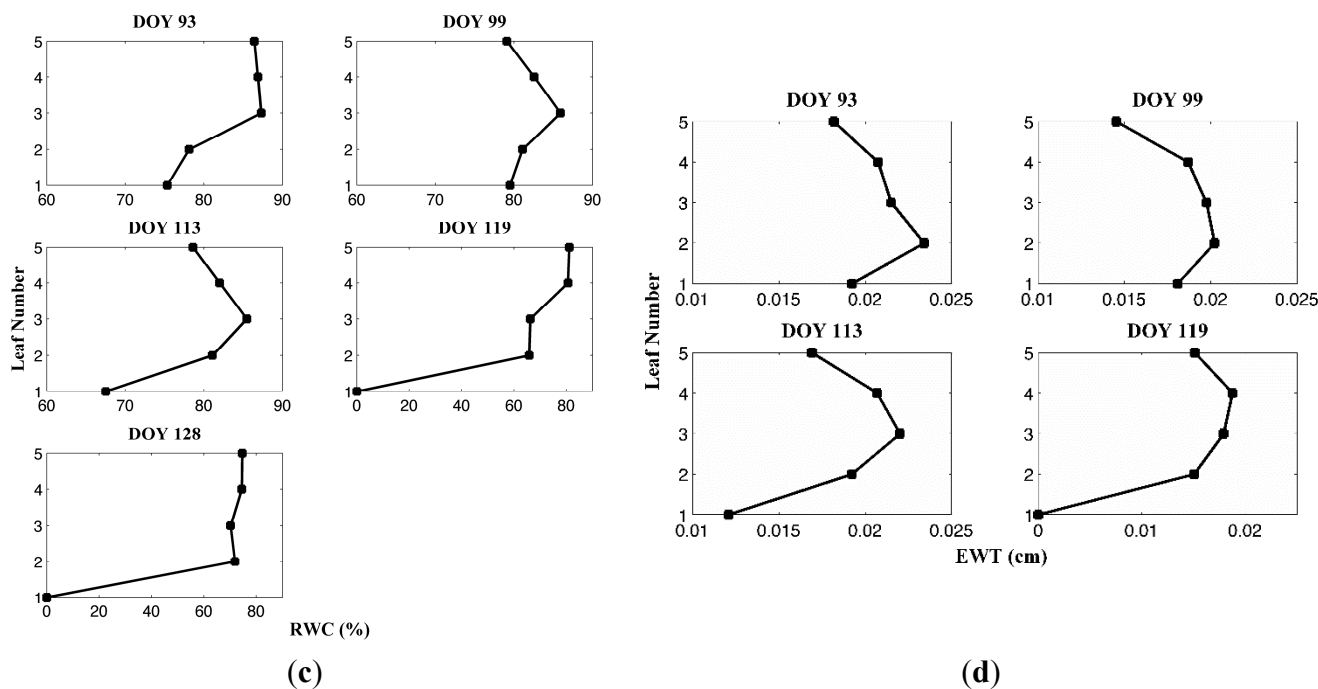


Figure 2. Leaf GWC_D (a), GWC_F (b), RWC (c), and EWT (d) averaged on each measurement date *versus* leaf number from the top (No.5 refers to the top leaf) to the bottom (No.1 refers to the bottom leaf) of the winter wheat canopy.

To understand the vertical distribution of leaf water-related properties of winter wheat, we plotted GWC_D , GWC_F , RWC, and EWT against the leaf number from the top to the bottom of the wheat canopy on each measurement date (Figure 2). The measurements taken on the same date were averaged for each leaf number. The pattern of the vertical distribution of GWC_D , GWC_F , RWC, and EWT were very similar. During the heading stage, the third leaf (the third and the fourth leaf for EWT) had higher values than the other top leaves. In the early ripening stage, the values of GWC_D , GWC_F , RWC, and EWT of all leaves were decreasing. The maximal value was usually found in the second leaf from the top of the canopy. The leaf water content of the fourth and the fifth leaves decreased rapidly, and especially the fifth leaf had dried out with minimal leaf water content that can hardly be detected.

3.2. Estimation of Water-Related Properties at Leaf Level

At leaf level, to determine which spectral bands of reflectance were sensitive to changes in leaf GWC_D , GWC_F , RWC, EWT, the linear correlation coefficients (r) were calculated for all wavelengths and plotted as correlograms (Figure 3). The correlograms showed no significant correlations between reflectance of the NIR region and RWC, EWT, but negative correlations between reflectance of the NIR region and GWC_D , GWC_F , though the correlations were not strong. All water-related properties demonstrated significant negative relationships with reflectance of the SWIR region, particularly around 1450, 1510, and 1860 nm. This result agreed with the findings of many studies that the stronger absorption bands of the SWIR region were more responsive to leaf water content variations than the weaker water absorption bands of the NIR region [8,42]. However, water absorption bands near 1450 and 1860 nm are strongly influenced by water vapor in the atmosphere so that they cannot be used for the aircraft- and satellite-based remote sensing. Therefore, we revised NDII and MSI by replacing the band sensitive to the change of water content with reflectance at 1510 nm.

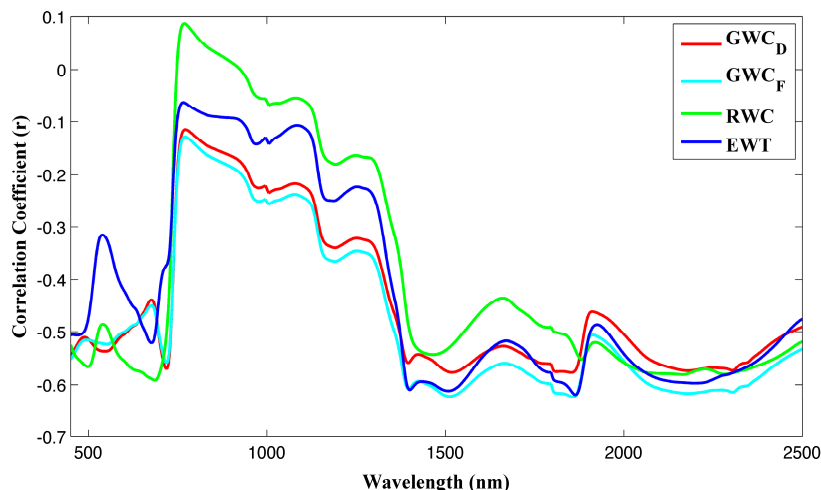


Figure 3. Correlations between reflectance at all wavelengths and GWC_D , GWC_F , RWC, EWT at leaf level of winter wheat. The significant correlation ($p < 0.001$) was indicated by r greater than 0.45 or less than -0.45 (140 samples).

We evaluated performances of both the existing VIs and the revised VIs in estimating water-related properties of winter wheat at leaf level. The relationships between VIs and GWC_D were nonlinear, fitted with exponential functions. The relationships between VIs and GWC_F , RWC can be described with linear functions. EWT was best retrieved by VIs using power functions. Table 5 shows R^2 and RMSE of the best-fit functions for each variable at leaf level. Given the number of samples (140 samples), the significant relationships for VIs ($p < 0.001$) were indicated by R^2 greater than 0.2.

Table 5. Statistics of the relationships between Vegetation Indexes (VIs) and gravimetric water content (GWC), relative water content (RWC), and equivalent water thickness (EWT) at leaf level of winter wheat. Given the number of samples (140 samples), the significant relationship ($p < 0.001$) was indicated by R^2 greater than 0.2.

| VIs | GWC_D | | GWC_F | | RWC (%) | | EWT (cm) | |
|---|---------|------|---------|------|---------|-------|----------|--------|
| | R^2 | RMSE | R^2 | RMSE | R^2 | RMSE | R^2 | RMSE |
| WI | 0.32 | 1.48 | 0.33 | 0.06 | 0.24 | 11.25 | 0.23 | 0.0036 |
| NDWI | 0.30 | 1.50 | 0.27 | 0.06 | 0.27 | 11.02 | 0.16 | 0.0038 |
| MSI | 0.45 | 1.33 | 0.43 | 0.06 | 0.26 | 11.08 | 0.33 | 0.0033 |
| NDII | 0.45 | 1.33 | 0.43 | 0.06 | 0.37 | 10.17 | 0.37 | 0.0032 |
| RMSI | 0.45 | 1.33 | 0.43 | 0.05 | 0.37 | 10.18 | 0.34 | 0.0032 |
| GVMi | 0.46 | 1.31 | 0.45 | 0.05 | 0.29 | 10.82 | 0.36 | 0.0032 |
| NDVI | 0.25 | 1.55 | 0.20 | 0.07 | 0.24 | 11.19 | 0.08 | 0.0040 |
| $CI_{red\ edge}$ | 0.30 | 1.49 | 0.26 | 0.06 | 0.25 | 11.13 | 0.05 | 0.0041 |
| NDMI | 0.30 | 1.50 | 0.26 | 0.06 | 0.28 | 10.91 | 0.18 | 0.0039 |
| NDII/NDMI | 0.02 | 1.77 | 0.01 | 0.07 | 0.06 | 12.50 | 0.01 | 0.0041 |
| $(\rho_{850} - \rho_{2218}) / (\rho_{850} - \rho_{1928})$ | 0.42 | 1.41 | 0.42 | 0.05 | 0.46 | 9.45 | 0.44 | 0.0027 |
| $(\rho_{850} - \rho_{1788}) / (\rho_{850} - \rho_{1928})$ | 0.43 | 1.39 | 0.41 | 0.05 | 0.39 | 10.05 | 0.41 | 0.0028 |
| $NDII_{1510}$ | 0.48 | 1.29 | 0.49 | 0.05 | 0.33 | 10.47 | 0.40 | 0.0028 |
| MSI_{1510} | 0.48 | 1.30 | 0.47 | 0.05 | 0.33 | 10.48 | 0.37 | 0.0032 |

At leaf level, the relationships between GWC_D , GWC_F and VIs were stronger than those for the other two variables. Overall, among different VIs, MSI NDII, RMSI, GVMi, $(\rho_{850} - \rho_{2218}) / (\rho_{850} - \rho_{1928})$, $(\rho_{850} - \rho_{1788}) / (\rho_{850} - \rho_{1928})$, and the revised NDII, MSI demonstrated better performances in predicting leaf-level water-related properties of winter wheat. In particular, $(\rho_{850} - \rho_{2218}) / (\rho_{850} - \rho_{1928})$ and $(\rho_{850} - \rho_{1788}) / (\rho_{850} - \rho_{1928})$ provided more accurate estimations of RWC and EWT than the other VIs. The significant relationships between four water-related properties and the revised NDII are illustrated in Figure 4. The exponential relationship between $NDII_{1510}$ and GWC_D implied that $NDII_{1510}$ were more sensitive to high values of GWC_D . $NDII_{1510}$ increased with the increase in GWC_F and EWT. The scattered relationship between $NDII_{1510}$ and RWC indicated that $NDII_{1510}$ was not as sensitive to the change in RWC as to the other variables, especially for low RWC values ranging from 45% to 70%.

NDVI and $CI_{red\ edge}$, which are sensitive to greenness of vegetation rather than water content, were not significantly related with EWT, but they had significant relationships with GWC_D , GWC_F , and RWC. Although some studies demonstrated significant relationships between GWC_D and NDII/NDMI [17,40], NDII/NDMI was not related to any of the measured variables in this study.

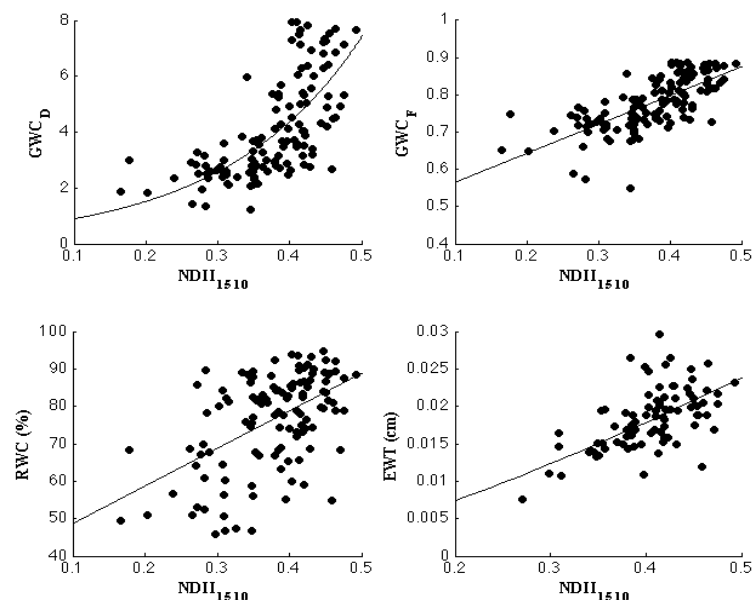


Figure 4. Relationships between $NDII_{1510}$ and GWC_D , GWC_F , RWC, EWT at leaf level of winter wheat.

To explore the vertical differences in the relationships between VIs and water-related properties at leaf level, we analyzed the relationships for each leaf layer from the top to the bottom of the canopy (Table 6). The relationships were not significant for the bottom leaf layer for all the water-related properties. For GWC_D and GWC_F , the second, third, and fourth leaf layers had stronger relationships than the top layer. For RWC, the stronger relationships were also found in the second, third, and fourth leaf layers, but the relationships were not significant for the top leaf layer. Although Table 5 shows less strong relationships between EWT and VIs than those for GWC_D and GWC_F , Table 6 shows stronger relationships between EWT and VIs for the top leaf layer than those of the other water-related properties. However, the relationships of EWT were less strong for intermediate leaf layers, and not significant for the bottom two leaf layers.

Table 6. Statistics of relationships between VIs and GWC_D (a), GWC_F (b), RWC (c), and EWT (d) for each leaf layer from the top (No.5 refers to the top leaf) to the bottom ((No.1 refers to the bottom leaf) of the winter wheat. Given the number of samples (28 samples), the significant relationships ($p < 0.001$) were indicated by R^2 values greater than 0.33.

| (a) GWC_D | | | | | | | | | | |
|---|-------------|-------|-------|-------|-------|-------|-------|-------|-------|-------|
| Vegetation Indexes | Leaf Number | | | | | | | | | |
| | 5 | | 4 | | 3 | | 2 | | 1 | |
| | R^2 | RMSE | R^2 | RMSE | R^2 | RMSE | R^2 | RMSE | R^2 | RMSE |
| WI | 0.13 | 1.47 | 0.32 | 1.40 | 0.54 | 1.44 | 0.36 | 1.54 | 0.01 | 1.66 |
| NDWI | 0.26 | 1.36 | 0.38 | 1.33 | 0.54 | 1.45 | 0.37 | 1.53 | 0.02 | 1.65 |
| MSI | 0.30 | 1.34 | 0.37 | 1.34 | 0.59 | 1.40 | 0.41 | 1.47 | 0.01 | 1.67 |
| NDII | 0.34 | 1.28 | 0.49 | 1.20 | 0.68 | 1.21 | 0.45 | 1.42 | 0.06 | 1.61 |
| RMSI | 0.34 | 1.28 | 0.50 | 1.19 | 0.67 | 1.22 | 0.44 | 1.43 | 0.06 | 1.62 |
| GVMi | 0.32 | 1.30 | 0.52 | 1.17 | 0.70 | 1.18 | 0.50 | 1.36 | 0.05 | 1.63 |
| NDVI | 0.41 | 1.21 | 0.43 | 1.27 | 0.68 | 1.20 | 0.25 | 1.66 | 0.03 | 1.65 |
| $CI_{red\ edge}$ | 0.49 | 1.13 | 0.52 | 1.17 | 0.71 | 1.15 | 0.17 | 1.75 | 0.06 | 1.62 |
| NDMI | 0.53 | 1.08 | 0.64 | 1.01 | 0.67 | 1.22 | 0.33 | 1.58 | 0.06 | 1.61 |
| NDII/NDMI | 0.25 | 1.37 | 0.04 | 1.65 | 0.25 | 1.85 | 0.01 | 1.92 | 0.01 | 1.65 |
| $(\rho_{850} - \rho_{2218}) / (\rho_{850} - \rho_{1928})$ | 0.31 | 1.31 | 0.49 | 1.20 | 0.66 | 1.25 | 0.36 | 1.50 | 0.08 | 1.60 |
| $(\rho_{850} - \rho_{1788}) / (\rho_{850} - \rho_{1928})$ | 0.23 | 1.38 | 0.44 | 1.27 | 0.66 | 1.24 | 0.44 | 1.41 | 0.17 | 1.52 |
| NDII ₁₅₁₀ | 0.39 | 1.23 | 0.48 | 1.21 | 0.70 | 1.17 | 0.43 | 1.45 | 0.03 | 1.64 |
| MSI ₁₅₁₀ | 0.38 | 1.24 | 0.47 | 1.23 | 0.70 | 1.17 | 0.44 | 1.44 | 0.03 | 1.65 |
| (b) GWC_F | | | | | | | | | | |
| Vegetation Indexes | Leaf Number | | | | | | | | | |
| | 5 | | 4 | | 3 | | 2 | | 1 | |
| | R^2 | RMSE | R^2 | RMSE | R^2 | RMSE | R^2 | RMSE | R^2 | RMSE |
| WI | 0.20 | 0.065 | 0.46 | 0.045 | 0.46 | 0.064 | 0.49 | 0.043 | 0.01 | 0.052 |
| NDWI | 0.32 | 0.060 | 0.49 | 0.044 | 0.43 | 0.065 | 0.53 | 0.042 | 0.04 | 0.051 |
| MSI | 0.34 | 0.059 | 0.48 | 0.044 | 0.48 | 0.063 | 0.54 | 0.041 | 0.01 | 0.052 |
| NDII | 0.36 | 0.058 | 0.57 | 0.040 | 0.56 | 0.057 | 0.58 | 0.039 | 0.04 | 0.051 |
| RMSI | 0.36 | 0.058 | 0.58 | 0.040 | 0.56 | 0.057 | 0.58 | 0.039 | 0.04 | 0.051 |
| GVMi | 0.36 | 0.058 | 0.59 | 0.039 | 0.59 | 0.056 | 0.64 | 0.037 | 0.05 | 0.051 |
| NDVI | 0.14 | 0.068 | 0.50 | 0.044 | 0.62 | 0.053 | 0.35 | 0.049 | 0.01 | 0.052 |
| $CI_{red\ edge}$ | 0.40 | 0.057 | 0.54 | 0.042 | 0.61 | 0.054 | 0.27 | 0.052 | 0.04 | 0.051 |
| NDMI | 0.46 | 0.054 | 0.61 | 0.039 | 0.55 | 0.058 | 0.41 | 0.047 | 0.02 | 0.051 |
| NDII/NDMI | 0.18 | 0.066 | 0.00 | 0.061 | 0.15 | 0.080 | 0.02 | 0.060 | 0.00 | 0.052 |
| $(\rho_{850} - \rho_{2218}) / (\rho_{850} - \rho_{1928})$ | 0.39 | 0.057 | 0.55 | 0.041 | 0.52 | 0.060 | 0.49 | 0.042 | 0.10 | 0.049 |
| $(\rho_{850} - \rho_{1788}) / (\rho_{850} - \rho_{1928})$ | 0.30 | 0.061 | 0.49 | 0.044 | 0.51 | 0.061 | 0.54 | 0.040 | 0.16 | 0.048 |
| NDII ₁₅₁₀ | 0.43 | 0.055 | 0.59 | 0.039 | 0.60 | 0.055 | 0.57 | 0.040 | 0.03 | 0.051 |
| MSI ₁₅₁₀ | 0.42 | 0.055 | 0.57 | 0.040 | 0.58 | 0.056 | 0.57 | 0.040 | 0.03 | 0.051 |

Table 6. Cont.

(c) RWC

| Vegetation Indexes | Leaf Number | | | | | | | | | |
|---|----------------|-------|----------------|-------|----------------|------|----------------|------|----------------|------|
| | 5 | | 4 | | 3 | | 2 | | 1 | |
| | R ² | RMSE | R ² | RMSE | R ² | RMSE | R ² | RMSE | R ² | RMSE |
| WI | 0.13 | 0.090 | 0.51 | 0.073 | 0.39 | 0.13 | 0.49 | 0.11 | 0.14 | 0.10 |
| NDWI | 0.16 | 0.086 | 0.35 | 0.085 | 0.31 | 0.14 | 0.56 | 0.10 | 0.08 | 0.10 |
| MSI | 0.23 | 0.083 | 0.53 | 0.072 | 0.51 | 0.12 | 0.46 | 0.11 | 0.01 | 0.11 |
| NDII | 0.20 | 0.085 | 0.50 | 0.074 | 0.53 | 0.11 | 0.59 | 0.10 | 0.03 | 0.11 |
| RMSI | 0.19 | 0.085 | 0.50 | 0.074 | 0.53 | 0.11 | 0.60 | 0.10 | 0.03 | 0.11 |
| GVMi | 0.22 | 0.083 | 0.54 | 0.072 | 0.55 | 0.11 | 0.61 | 0.10 | 0.01 | 0.11 |
| NDVI | 0.00 | 0.094 | 0.37 | 0.083 | 0.39 | 0.13 | 0.51 | 0.11 | 0.11 | 0.10 |
| CI _{red edge} | 0.07 | 0.091 | 0.33 | 0.086 | 0.45 | 0.12 | 0.42 | 0.12 | 0.07 | 0.10 |
| NDMI | 0.08 | 0.090 | 0.39 | 0.082 | 0.45 | 0.12 | 0.51 | 0.11 | 0.07 | 0.10 |
| NDII/NDMI | 0.00 | 0.094 | 0.01 | 0.105 | 0.10 | 0.16 | 0.00 | 0.15 | 0.08 | 0.10 |
| $(\rho_{850} - \rho_{2218}) / (\rho_{850} - \rho_{1928})$ | 0.32 | 0.078 | 0.58 | 0.069 | 0.61 | 0.10 | 0.41 | 0.12 | 0.07 | 0.10 |
| $(\rho_{850} - \rho_{1788}) / (\rho_{850} - \rho_{1928})$ | 0.23 | 0.083 | 0.53 | 0.072 | 0.59 | 0.11 | 0.50 | 0.11 | 0.03 | 0.11 |
| NDII ₁₅₁₀ | 0.23 | 0.083 | 0.53 | 0.072 | 0.54 | 0.11 | 0.53 | 0.11 | 0.02 | 0.11 |
| MSI ₁₅₁₀ | 0.23 | 0.083 | 0.53 | 0.072 | 0.53 | 0.11 | 0.52 | 0.11 | 0.02 | 0.11 |

(d) EWT

| Vegetation Indexes | Leaf Number | | | | | | | | | |
|---|----------------|-------|----------------|-------|----------------|-------|----------------|-------|----------------|-------|
| | 5 | | 4 | | 3 | | 2 | | 1 | |
| | R ² | RMSE |
| WI | 0.55 | 0.003 | 0.25 | 0.003 | 0.28 | 0.003 | 0.17 | 0.004 | 0.01 | 0.004 |
| NDWI | 0.68 | 0.002 | 0.38 | 0.003 | 0.18 | 0.003 | 0.17 | 0.004 | 0.02 | 0.004 |
| MSI | 0.61 | 0.002 | 0.35 | 0.003 | 0.35 | 0.003 | 0.23 | 0.004 | 0.04 | 0.004 |
| NDII | 0.62 | 0.002 | 0.35 | 0.003 | 0.36 | 0.003 | 0.17 | 0.004 | 0.02 | 0.004 |
| RMSI | 0.62 | 0.002 | 0.32 | 0.003 | 0.35 | 0.003 | 0.17 | 0.004 | 0.01 | 0.004 |
| GVMi | 0.62 | 0.002 | 0.32 | 0.003 | 0.33 | 0.003 | 0.23 | 0.004 | 0.16 | 0.003 |
| NDVI | 0.44 | 0.002 | 0.32 | 0.003 | 0.38 | 0.003 | 0.18 | 0.004 | 0.02 | 0.004 |
| CI _{red edge} | 0.45 | 0.002 | 0.32 | 0.002 | 0.36 | 0.003 | 0.08 | 0.004 | 0.06 | 0.004 |
| NDMI | 0.37 | 0.002 | 0.27 | 0.003 | 0.26 | 0.004 | 0.26 | 0.004 | 0.03 | 0.004 |
| NDII/NDMI | 0.03 | 0.003 | 0.12 | 0.003 | 0.24 | 0.004 | 0.24 | 0.004 | 0.22 | 0.003 |
| $(\rho_{850} - \rho_{2218}) / (\rho_{850} - \rho_{1928})$ | 0.76 | 0.001 | 0.45 | 0.002 | 0.41 | 0.003 | 0.27 | 0.003 | 0.17 | 0.003 |
| $(\rho_{850} - \rho_{1788}) / (\rho_{850} - \rho_{1928})$ | 0.75 | 0.001 | 0.38 | 0.003 | 0.43 | 0.003 | 0.25 | 0.004 | 0.16 | 0.003 |
| NDII ₁₅₁₀ | 0.68 | 0.002 | 0.39 | 0.003 | 0.40 | 0.003 | 0.28 | 0.003 | 0.02 | 0.004 |
| MSI ₁₅₁₀ | 0.67 | 0.002 | 0.39 | 0.003 | 0.40 | 0.003 | 0.26 | 0.004 | 0.02 | 0.004 |

3.3. Water-Related Properties within a Winter Wheat Canopy

GWC_D, GWC_F, RWC, and EWT for the cumulative leaf number within a winter wheat canopy are illustrated in Figure 5. For GWC_D, GWC_F, and EWT, the values were minimal at the top of the canopy, progressively increasing, reaching maximum values, and then remaining stable or slightly decreased. RWC demonstrated a slightly different pattern. RWC for the cumulative leaf number increased slightly from the top leaf to the intermediate position of the canopy, and then decreased progressively, reaching the minimal value when including the bottom leaf.

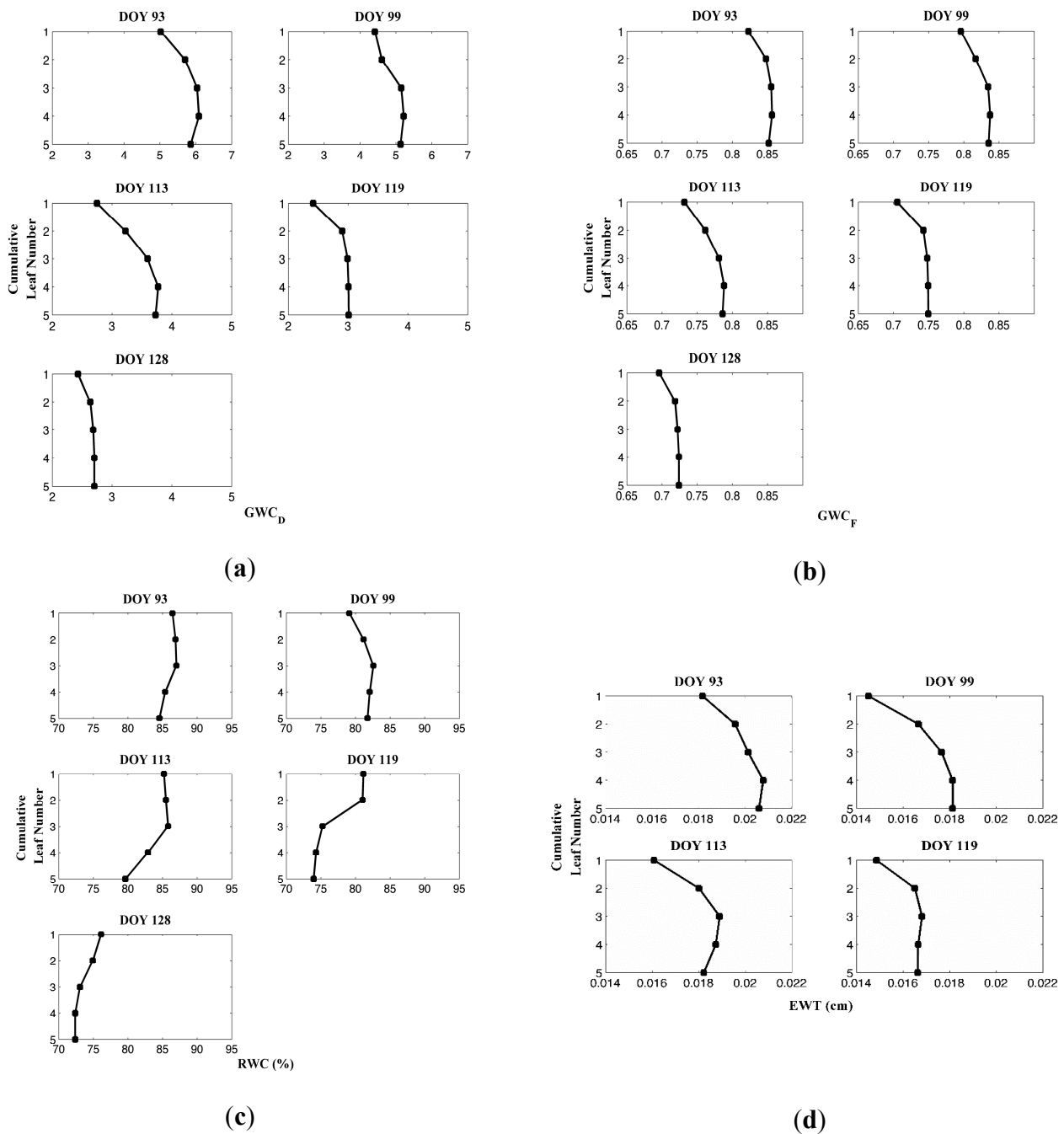


Figure 5. GWC_D (a), GWC_F (b), RWC (c), and EWT (d) for the cumulative leaf number within a winter wheat canopy. Cumulative leaf number 1 corresponds to the top leaf (leaf No. 5), and cumulative leaf number 5 corresponds to the top five leaves, from the top leaf (leaf No. 5) to the bottom leaf (leaf No. 1) of the canopy.

Importantly, the leaf position at which water-related properties for the cumulative leaf number reached the maximum varied with the growth stages. During the heading stage, the maximal values occurred at the top three or four leaves, but during the ripening stage, water-related properties reached maximum values at the top two leaves.

3.4. Estimations of Water-Related Properties at Canopy Level

To determine the wavelengths that are sensitive to the water-related properties for the cumulative leaf number within the canopy, we evaluated the relationships between canopy reflectance at all wavelengths and water-related properties for the cumulative leaf number within the winter wheat canopy. The correlograms of GWC_D , GWC_F , RWC, and EWT (Figure 6) illustrated that all water-related properties were positively correlated with reflectance of the NIR region but negatively correlated with reflectance of the VIS and SWIR regions. The relationships between canopy reflectance and RWC and EWT were less strong than those of GWC_D , GWC_F . The strongest positive relationship was found around 750 nm and the strongest negative relationship was found around 670, 1955, and 2020 nm. The varying relationships between reflectance and GWC_D and GWC_F for the cumulative leaf number were obvious in the VIS and SWIR regions, where the top leaf had the lower correlation and the top three leaves had the stronger correlation with reflectance. Such varying relationships were more pronounced for RWC and EWT. Based on these observations, we revised NDII and MSI by replacing the water absorption bands with reflectance at 2020 nm, because 1955 nm was close to the noisy bands.

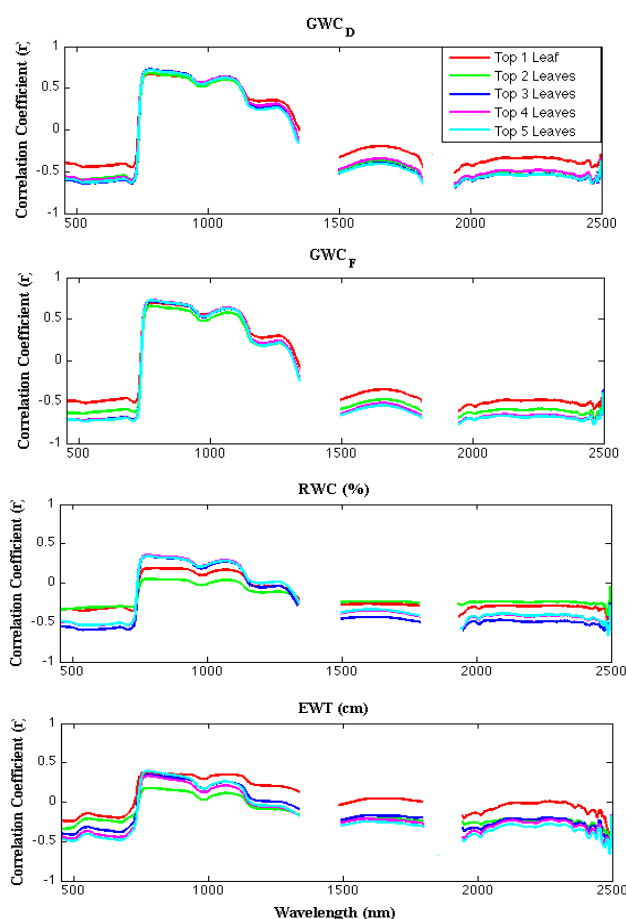


Figure 6. Correlation between canopy reflectance at all wavelengths and GWC_D , GWC_F , RWC, and EWT for the cumulative leaf number. Top one leaf corresponds to leaf No. 5, and top five leaves correspond to the leaf No.5 to leaf No.1. The significant correlation ($p < 0.001$) was indicated by r greater than 0.52 or less than -0.52 (33 samples).

To determine the position of leaf number at which VIs can best retrieve canopy water-related properties of winter wheat, we evaluated the relationships between different VIs and GWC_D , GWC_F , RWC, and EWT for the cumulative leaf number. Table 7 summarizes the statistics of relationships between studied VIs and water-related properties at canopy level. For GWC_D and GWC_F , relationships were significant for all studied VIs except NDMI and NDII/NDMI. These VIs can sense the canopy GWC_D and GWC_F of the top two, three, four, and five leaves. The most accurate estimations of GWC_D and GWC_F were achieved for the top three leaves. The revised NDII and MSI did not improve the estimations of GWC_D and GWC_F obviously compared with the existing water absorption-based VIs. The relationships between studied VIs and RWC and EWT for the cumulative leaf number were not significant. However, the revised NDII and MSI provided more accurate estimations of RWC and EWT than the existing VIs, and the most accurate estimations were achieved for the top three and four leaves for RWC and for the top four and five leaves for EWT.

Table 7. Statistics of relationships between VIs based on canopy reflectance and GWC_D (a), GWC_F (b), RWC (c), and EWT (d) for the cumulative leaf number within the winter wheat canopy. The significant relationships ($p < 0.001$) were indicated by R^2 values greater than 0.29 (33 samples).

| (a) GWC_D | | | | | | | | | | |
|------------------------|------------------------|------|-------|------|-------|------|-------|------|-------|------|
| Vegetation Indexes | Cumulative Leaf Number | | | | | | | | | |
| | Top 1 | | Top 2 | | Top 3 | | Top 4 | | Top 5 | |
| | R^2 | RMSE | R^2 | RMSE | R^2 | RMSE | R^2 | RMSE | R^2 | RMSE |
| WI | 0.53 | 1.06 | 0.59 | 0.90 | 0.65 | 0.94 | 0.60 | 1.00 | 0.60 | 0.94 |
| NDWI | 0.52 | 1.07 | 0.58 | 0.91 | 0.65 | 0.93 | 0.61 | 0.98 | 0.62 | 0.92 |
| MSI | 0.48 | 1.11 | 0.53 | 0.97 | 0.60 | 1.00 | 0.59 | 1.01 | 0.60 | 0.94 |
| NDII | 0.46 | 1.13 | 0.53 | 0.97 | 0.60 | 1.00 | 0.57 | 1.03 | 0.58 | 0.96 |
| RMSI | 0.48 | 1.11 | 0.53 | 0.97 | 0.59 | 1.01 | 0.56 | 1.05 | 0.57 | 0.98 |
| GVMi | 0.45 | 1.15 | 0.52 | 0.98 | 0.59 | 1.01 | 0.57 | 1.04 | 0.58 | 0.97 |
| NDVI | 0.36 | 1.23 | 0.48 | 1.02 | 0.57 | 1.04 | 0.56 | 1.04 | 0.56 | 0.98 |
| CI _{red edge} | 0.56 | 1.03 | 0.63 | 0.86 | 0.70 | 0.86 | 0.67 | 0.91 | 0.66 | 0.86 |
| NDMI | 0.26 | 1.33 | 0.27 | 1.21 | 0.31 | 1.31 | 0.30 | 1.32 | 0.31 | 1.23 |
| NDII/NDMI | 0.00 | 1.54 | 0.01 | 1.40 | 0.02 | 1.56 | 0.02 | 1.56 | 0.02 | 1.47 |
| NDII ₂₀₂₀ | 0.41 | 1.18 | 0.55 | 0.92 | 0.63 | 0.96 | 0.61 | 0.98 | 0.62 | 0.92 |
| MSI ₂₀₂₀ | 0.45 | 1.15 | 0.55 | 0.92 | 0.63 | 0.96 | 0.60 | 1.00 | 0.61 | 0.93 |

| (b) GWC_F | | | | | | | | | | |
|-----------------------|------------------------|------|-------|------|-------|------|-------|------|-------|------|
| Vegetation Indexes | Cumulative Leaf Number | | | | | | | | | |
| | Top 1 | | Top 2 | | Top 3 | | Top 4 | | Top 5 | |
| | R^2 | RMSE | R^2 | RMSE | R^2 | RMSE | R^2 | RMSE | R^2 | RMSE |
| WI | 0.48 | 0.05 | 0.57 | 0.04 | 0.61 | 0.04 | 0.60 | 0.04 | 0.59 | 0.04 |
| NDWI | 0.45 | 0.05 | 0.54 | 0.04 | 0.60 | 0.04 | 0.59 | 0.04 | 0.59 | 0.04 |
| MSI | 0.37 | 0.06 | 0.50 | 0.04 | 0.55 | 0.04 | 0.55 | 0.04 | 0.55 | 0.04 |
| NDII | 0.37 | 0.06 | 0.49 | 0.04 | 0.55 | 0.04 | 0.55 | 0.04 | 0.55 | 0.04 |
| RMSI | 0.41 | 0.05 | 0.52 | 0.04 | 0.57 | 0.04 | 0.57 | 0.04 | 0.57 | 0.04 |
| GVMi | 0.37 | 0.06 | 0.50 | 0.04 | 0.55 | 0.04 | 0.56 | 0.04 | 0.56 | 0.04 |
| NDVI | 0.27 | 0.06 | 0.42 | 0.04 | 0.50 | 0.04 | 0.52 | 0.04 | 0.52 | 0.04 |

Table 7. Cont.

| Vegetation Indexes | Cumulative Leaf Number | | | | | | | | | |
|------------------------|------------------------|--------|----------------|--------|----------------|--------|----------------|--------|----------------|--------|
| | Top 1 | | Top 2 | | Top 3 | | Top 4 | | Top 5 | |
| | R ² | RMSE | R ² | RMSE | R ² | RMSE | R ² | RMSE | R ² | RMSE |
| CI _{red edge} | 0.48 | 0.05 | 0.59 | 0.04 | 0.65 | 0.04 | 0.64 | 0.04 | 0.63 | 0.04 |
| NDMI | 0.22 | 0.06 | 0.24 | 0.05 | 0.25 | 0.05 | 0.24 | 0.05 | 0.24 | 0.05 |
| NDII/NDMI | 0.00 | 0.07 | 0.02 | 0.06 | 0.03 | 0.06 | 0.03 | 0.06 | 0.03 | 0.06 |
| NDII ₂₀₂₀ | 0.32 | 0.06 | 0.49 | 0.04 | 0.55 | 0.04 | 0.56 | 0.04 | 0.57 | 0.04 |
| MSI ₂₀₂₀ | 0.31 | 0.06 | 0.48 | 0.04 | 0.54 | 0.05 | 0.56 | 0.04 | 0.56 | 0.04 |
| (c) RWC | | | | | | | | | | |
| Vegetation Indexes | Cumulative Leaf Number | | | | | | | | | |
| | Top 1 | | Top 2 | | Top 3 | | Top 4 | | Top 5 | |
| | R ² | RMSE | R ² | RMSE | R ² | RMSE | R ² | RMSE | R ² | RMSE |
| WI | 0.02 | 7.88 | 0.07 | 6.50 | 0.27 | 7.21 | 0.25 | 7.16 | 0.21 | 7.18 |
| NDWI | 0.02 | 7.88 | 0.07 | 6.50 | 0.29 | 7.12 | 0.27 | 7.06 | 0.23 | 7.07 |
| MSI | 0.02 | 7.87 | 0.07 | 6.49 | 0.27 | 7.24 | 0.26 | 7.14 | 0.22 | 7.13 |
| NDII | 0.02 | 7.86 | 0.08 | 6.44 | 0.27 | 7.20 | 0.26 | 7.12 | 0.22 | 7.12 |
| RMSI | 0.01 | 7.89 | 0.07 | 6.49 | 0.27 | 7.24 | 0.26 | 7.14 | 0.22 | 7.15 |
| GVMi | 0.02 | 7.87 | 0.08 | 6.45 | 0.27 | 7.24 | 0.26 | 7.14 | 0.22 | 7.14 |
| NDVI | 0.03 | 7.83 | 0.13 | 6.28 | 0.28 | 7.17 | 0.25 | 7.17 | 0.22 | 7.12 |
| CI _{red edge} | 0.04 | 7.80 | 0.10 | 6.38 | 0.31 | 7.00 | 0.30 | 6.95 | 0.26 | 6.97 |
| NDMI | 0.01 | 7.92 | 0.00 | 6.72 | 0.15 | 7.78 | 0.13 | 7.74 | 0.14 | 7.49 |
| NDII/NDMI | 0.02 | 7.86 | 0.03 | 6.62 | 0.01 | 8.41 | 0.02 | 8.21 | 0.00 | 8.06 |
| NDII ₂₀₂₀ | 0.09 | 7.08 | 0.22 | 5.21 | 0.33 | 6.81 | 0.34 | 6.50 | 0.30 | 6.36 |
| MSI ₂₀₂₀ | 0.10 | 7.05 | 0.23 | 5.14 | 0.33 | 6.81 | 0.34 | 6.50 | 0.31 | 6.23 |
| (d) EWT | | | | | | | | | | |
| Vegetation Indexes | Cumulative Leaf Number | | | | | | | | | |
| | Top 1 | | Top 2 | | Top 3 | | Top 4 | | Top 5 | |
| | R ² | RMSE | R ² | RMSE | R ² | RMSE | R ² | RMSE | R ² | RMSE |
| WI | 0.07 | 0.0028 | 0.12 | 0.0027 | 0.26 | 0.0024 | 0.26 | 0.0024 | 0.29 | 0.0023 |
| NDWI | 0.05 | 0.0028 | 0.09 | 0.0027 | 0.24 | 0.0024 | 0.26 | 0.0024 | 0.29 | 0.0023 |
| MSI | 0.06 | 0.0028 | 0.08 | 0.0028 | 0.22 | 0.0024 | 0.22 | 0.0025 | 0.25 | 0.0023 |
| NDII | 0.05 | 0.0028 | 0.08 | 0.0028 | 0.22 | 0.0024 | 0.22 | 0.0025 | 0.25 | 0.0023 |
| RMSI | 0.06 | 0.0028 | 0.08 | 0.0028 | 0.22 | 0.0024 | 0.22 | 0.0025 | 0.25 | 0.0023 |
| GVMi | 0.05 | 0.0029 | 0.08 | 0.0028 | 0.22 | 0.0024 | 0.23 | 0.0024 | 0.26 | 0.0023 |
| NDVI | 0.07 | 0.0028 | 0.07 | 0.0028 | 0.22 | 0.0024 | 0.25 | 0.0024 | 0.27 | 0.0023 |
| CI _{red edge} | 0.05 | 0.0028 | 0.07 | 0.0028 | 0.19 | 0.0025 | 0.20 | 0.0025 | 0.23 | 0.0024 |
| NDMI | 0.21 | 0.0026 | 0.13 | 0.0027 | 0.14 | 0.0025 | 0.14 | 0.0026 | 0.15 | 0.0025 |
| NDII/NDMI | 0.16 | 0.0027 | 0.20 | 0.0026 | 0.17 | 0.0025 | 0.18 | 0.0025 | 0.20 | 0.0024 |
| NDII ₂₀₂₀ | 0.04 | 0.0028 | 0.33 | 0.0019 | 0.39 | 0.0066 | 0.40 | 0.0064 | 0.41 | 0.0064 |
| MSI ₂₀₂₀ | 0.05 | 0.0028 | 0.34 | 0.0019 | 0.41 | 0.0065 | 0.42 | 0.0064 | 0.42 | 0.0063 |

4. Discussion

4.1. The Vertical Distribution of Water Content within a Winter Wheat Canopy

In this study, we evaluated the vertical distribution of four water-related properties (GWC_D , GWC_F , RWC, and EWT) within a winter wheat canopy during heading and early ripening stages. Our analysis showed that the vertical distribution of GWC_D , GWC_F , RWC, and EWT followed a near-bell-shaped curve with the highest values at the intermediate leaf position and the lowest value at the bottom leaf. After the emergence of the flag leaf (the top leaf), it contributes to the major part of photosynthesis and transpiration of wheat canopy. Since the flag leaf may consume more water through evapotranspiration, it contained less water than the intermediate leaves.

The vertical profile directly affected water-related properties for the cumulative leaf number within the winter wheat canopy. Our analysis demonstrated that water-related properties for the cumulative leaf number progressively increased, reaching maximum values at the intermediate leaf position, and then remained stable (such as GWC_D and GWC_F) or slightly decreased (such as RWC and EWT). Results implied that for GWC_D and GWC_F , the values of the top three or four leaves and the values of the top two or three leaves can represent GWC of the whole canopy during the heading stage and the early ripening stage, respectively. As for RWC and EWT, since they were more variable along the vertical profile than GWC_D and GWC_F , RWC and EWT of the whole canopy should be calculated based on the top four leaves or all leaves.

4.2. Estimations of Leaf and Canopy Water Content with Consideration of Vertical Distributions of Water-Related Properties

At leaf level, the analysis demonstrated strong relationships between EWT and VIs for the top leaf layer, with R^2 values ranging from 0.60–0.76 for water-related VIs, similar to the results shown in some other studies [8,43]. On the other hand, for GWC_D , GWC_F , and RWC, the strongest relationships with VIs were found in the intermediate leaf layers. The vertical differences in the relationships between VIs and water-related properties of winter wheat at leaf level indicated that the uniform model to estimate leaf water-related properties with remote sensing VIs might result in errors, particularly for vegetation with complex vertical architecture.

At canopy level, water absorption- and greenness-based VIs provided the most accurate estimations of GWC_D and GWC_F for the top three or four leaves (Figure 7). As GWC_D and GWC_F of the top three or four leaves can represent GWC of the whole canopy, these water absorption- and greenness-based VIs can be used to retrieve GWC of winter wheat. It was interesting that NDVI and $CI_{red\ edge}$ provided as accurate estimation of GWC as the water absorption-based VIs did at canopy level. These observations agreed with the findings that greenness indices were used to track seasonality of GWC in grassland and savanna because plant water status affects LAI and chlorophyll content [6].

Based on our results, the studied VIs were not feasible to accurately estimate canopy RWC of winter wheat during heading and early ripening stages. Although the revised NDII and MSI provided the best estimation of RWC for the top four leaves (Figure 7), the R^2 value was still quite low to indicate a convincing relationship between the revised NDII, MSI and RWC for the cumulative leaf number within the winter wheat canopy. The fact that VIs based on the reflectance of NIR and/or SWIR region were not

suitable for RWC estimations has been discussed in many studies [44,45]. These studies suggested that it was not feasible to detect RWC within the biologically meaningful range as the relative small changes in leaf water content associated with large changes in turgor pressure.

The poor relationships between the existing VIs and EWT for the cumulative leaf number at canopy level were different from some other EWT estimation studies. We hypothesized that there might be two reasons for the poor relationships. First, EWT calculated in this study described the mean leaf EWT at canopy level. Due to the lack of LAI measurements, the EWT for the cumulative leaf number did not take into account the impact of LAI. However, studies have shown that a large variability of LAI may cancel out water-related features in reflectance [46,47] and thus complicates the estimation of mean leaf EWT at canopy level. Second, while the relationships between the existing VIs and EWT were weak, the revised NDII and MSI provided more accurate estimations of EWT for the cumulative leaf number. Particularly, the best estimation was achieved for EWT of the top four and five leaves (Figure 7). These findings suggested that water absorption-based VIs were able to estimate EWT of winter wheat, but the suitable bands sensitive to water absorptions should be carefully selected for the studied species.

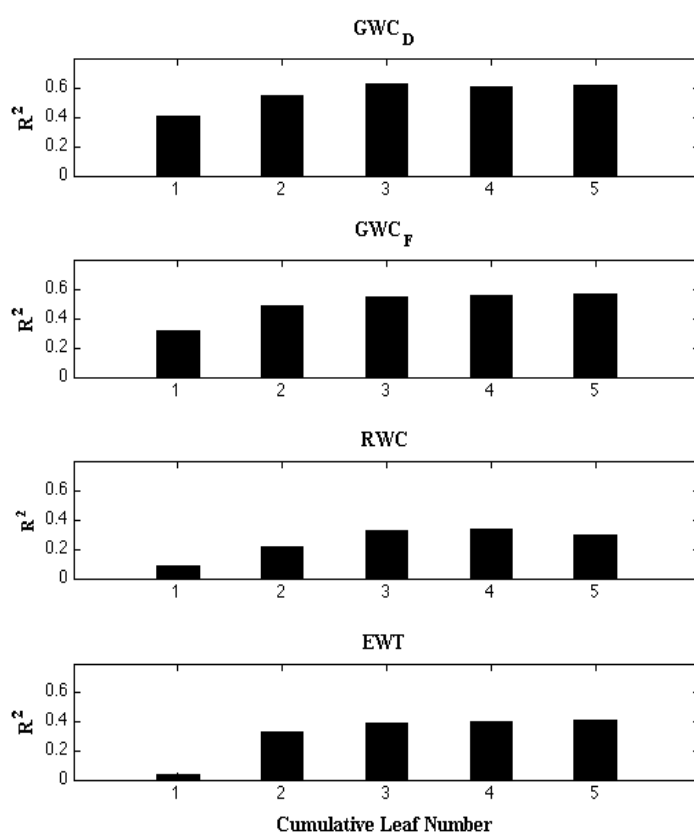


Figure 7. R^2 for the relationships between NDII₂₀₂₀ and water-related properties for the cumulative leaf number.

In order to gain a better understanding of how ‘deep’ remote sensing VIs derived from canopy spectra can ‘penetrate’ the winter wheat canopy and provide estimations of water-related properties as shown in the results of this study, we assessed if canopy spectra without the effects of varying plant geometries would show the similar results. We simulated canopy spectra using PROSPECT+SAILH

model based on the cumulative measurements of chlorophyll content, EWT, leaf dry matter, and LAI for the top one to top five leaves, respectively. Leaf chlorophyll content was measured in the field using SPAD-502 chlorophyll meter (Minolta, Valencia, Spain), the SPAD values were then converted to chlorophyll content (g/cm^2) according to the equation [48]. Due to a lack of LAI measurements, we assumed that LAI was calculated as the cumulative leaf area along the vertical structure divided by ground area of $6 \text{ cm} \times 6 \text{ cm}$, so that LAI was kept in the reasonable range (between 3 and 5 during the heading stage with a five-leaf vertical structure). The simulations showed that canopy spectra simulated with the cumulative values of the top five leaves were closest to the canopy spectra measured in the field, with the least mean RMSE between the measured and the simulated canopy spectra (Figure 8), while the simulated spectra for the top three and four leaves also had low RMSE values. We then evaluated the position of leaf number at which VIs can best retrieve canopy water-related properties of winter wheat by analyzing the relationships between VIs derived from the simulated spectra for the top five leaves and water-related properties for the cumulative leaf numbers. Overall, the simulated VIs showed stronger relationships with water-related properties than VIs derived from the measured canopy spectra (Table 8), implying that the accuracy of water-related properties (EWT in particular) estimations were affected by plant geometries. The relationships between water-related properties and the simulated VIs demonstrated the similar results that the studied VIs provided the most accurate estimations of GWC_D , GWC_F , and RWC for the top three leaves, and the most accurate estimation of EWT for the top four and five leaves. Since GWC_D , GWC_F , and RWC values of the top three leaves, and EWT values of the top four and five leaves can represent water status for the whole canopy, the findings of this study suggested that water-related properties of winter wheat estimated from VIs could represent the water status of the whole canopy.

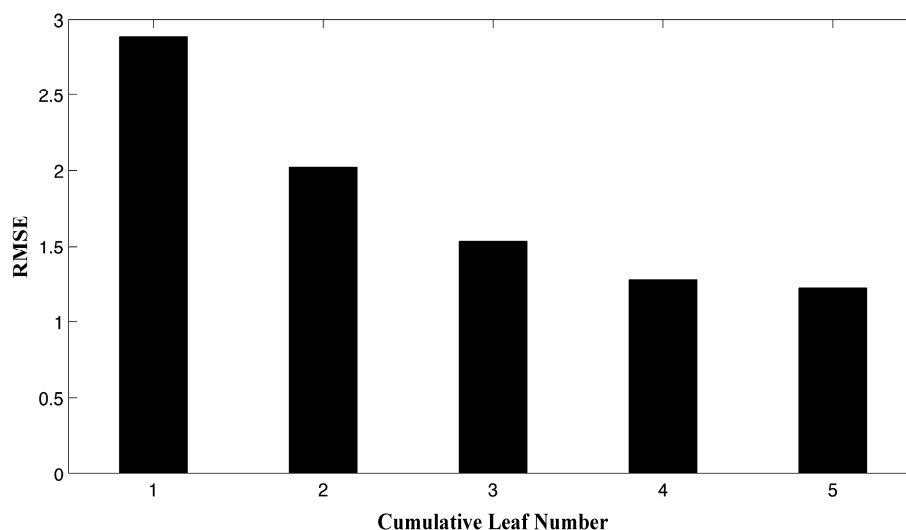


Figure 8. Mean RMSE between the measured canopy spectra and the canopy spectra simulated with PROSPECT+SAILH model for the top one, two, three, four, and five leaves, respectively.

Table 8. Statistics of relationships between VIs based on canopy reflectance and GWC_D (a), GWC_F (b), RWC (c), and EWT (d) for the cumulative leaf number within the winter wheat canopy. The significant relationships ($p < 0.001$) were indicated by R² values greater than 0.29 (33 samples).

| (a) GWC _D | | | | | | | | | | |
|------------------------|------------------------|------|----------------|------|----------------|------|----------------|------|----------------|------|
| Vegetation Indexes | Cumulative Leaf Number | | | | | | | | | |
| | Top 1 | | Top 2 | | Top 3 | | Top 4 | | Top 5 | |
| | R ² | RMSE | R ² | RMSE | R ² | RMSE | R ² | RMSE | R ² | RMSE |
| WI | 0.50 | 1.11 | 0.74 | 0.72 | 0.77 | 0.77 | 0.73 | 0.83 | 0.75 | 0.75 |
| NDWI | 0.46 | 1.16 | 0.69 | 0.80 | 0.73 | 0.83 | 0.70 | 0.87 | 0.71 | 0.80 |
| MSI | 0.44 | 1.18 | 0.66 | 0.83 | 0.70 | 0.88 | 0.67 | 0.92 | 0.67 | 0.85 |
| NDII | 0.47 | 1.14 | 0.69 | 0.79 | 0.73 | 0.83 | 0.70 | 0.88 | 0.71 | 0.81 |
| RMSI | 0.48 | 1.13 | 0.72 | 0.76 | 0.74 | 0.82 | 0.69 | 0.88 | 0.71 | 0.80 |
| GVMi | 0.50 | 1.12 | 0.72 | 0.75 | 0.74 | 0.81 | 0.70 | 0.87 | 0.71 | 0.80 |
| NDVI | 0.28 | 1.34 | 0.43 | 1.07 | 0.51 | 1.11 | 0.50 | 1.12 | 0.50 | 1.05 |
| CI _{red edge} | 0.43 | 1.19 | 0.59 | 0.92 | 0.62 | 0.98 | 0.55 | 1.07 | 0.55 | 0.99 |
| NDMI | 0.20 | 1.37 | 0.24 | 1.35 | 0.29 | 1.33 | 0.29 | 1.33 | 0.29 | 1.33 |
| NDII/NDMI | 0.29 | 1.33 | 0.33 | 1.22 | 0.36 | 1.20 | 0.35 | 1.20 | 0.37 | 1.19 |
| NDII ₂₀₂₀ | 0.32 | 1.30 | 0.50 | 1.00 | 0.57 | 1.05 | 0.56 | 1.06 | 0.55 | 1.00 |
| MSI ₂₀₂₀ | 0.34 | 1.28 | 0.53 | 0.97 | 0.60 | 1.01 | 0.58 | 1.02 | 0.58 | 0.96 |

| (b) GWC _F | | | | | | | | | | |
|------------------------|------------------------|------|----------------|------|----------------|------|----------------|------|----------------|------|
| Vegetation Indexes | Cumulative Leaf Number | | | | | | | | | |
| | Top 1 | | Top 2 | | Top 3 | | Top 4 | | Top 5 | |
| | R ² | RMSE | R ² | RMSE | R ² | RMSE | R ² | RMSE | R ² | RMSE |
| WI | 0.45 | 0.05 | 0.73 | 0.03 | 0.71 | 0.03 | 0.70 | 0.03 | 0.71 | 0.03 |
| NDWI | 0.36 | 0.05 | 0.63 | 0.03 | 0.63 | 0.04 | 0.63 | 0.04 | 0.63 | 0.03 |
| MSI | 0.33 | 0.06 | 0.58 | 0.04 | 0.57 | 0.04 | 0.57 | 0.04 | 0.57 | 0.04 |
| NDII | 0.37 | 0.05 | 0.64 | 0.03 | 0.62 | 0.04 | 0.62 | 0.04 | 0.62 | 0.04 |
| RMSI | 0.44 | 0.05 | 0.69 | 0.03 | 0.67 | 0.03 | 0.66 | 0.03 | 0.67 | 0.03 |
| GVMi | 0.42 | 0.05 | 0.68 | 0.03 | 0.65 | 0.04 | 0.64 | 0.04 | 0.64 | 0.03 |
| NDVI | 0.16 | 0.06 | 0.36 | 0.04 | 0.39 | 0.05 | 0.40 | 0.05 | 0.40 | 0.04 |
| CI _{red edge} | 0.43 | 0.05 | 0.57 | 0.04 | 0.58 | 0.04 | 0.54 | 0.04 | 0.54 | 0.04 |
| NDMI | 0.25 | 0.06 | 0.37 | 0.05 | 0.36 | 0.05 | 0.37 | 0.05 | 0.37 | 0.05 |
| NDII/NDMI | 0.23 | 0.06 | 0.36 | 0.05 | 0.36 | 0.05 | 0.33 | 0.06 | 0.34 | 0.06 |
| NDII ₂₀₂₀ | 0.19 | 0.06 | 0.40 | 0.04 | 0.41 | 0.05 | 0.42 | 0.05 | 0.42 | 0.04 |
| MSI ₂₀₂₀ | 0.21 | 0.06 | 0.43 | 0.04 | 0.45 | 0.04 | 0.45 | 0.04 | 0.45 | 0.04 |

| (c) RWC | | | | | | | | | | |
|--------------------|------------------------|------|----------------|------|----------------|------|----------------|------|----------------|------|
| Vegetation Indexes | Cumulative Leaf Number | | | | | | | | | |
| | Top 1 | | Top 2 | | Top 3 | | Top 4 | | Top 5 | |
| | R ² | RMSE | R ² | RMSE | R ² | RMSE | R ² | RMSE | R ² | RMSE |
| WI | 0.05 | 7.24 | 0.23 | 6.32 | 0.42 | 6.27 | 0.42 | 6.22 | 0.39 | 6.22 |
| NDWI | 0.04 | 7.30 | 0.22 | 6.35 | 0.36 | 6.58 | 0.36 | 6.56 | 0.33 | 6.53 |
| MSI | 0.04 | 7.28 | 0.25 | 6.24 | 0.39 | 6.44 | 0.38 | 6.46 | 0.35 | 6.42 |
| NDII | 0.04 | 7.27 | 0.24 | 6.26 | 0.40 | 6.38 | 0.39 | 6.37 | 0.37 | 6.35 |
| RMSI | 0.05 | 7.24 | 0.23 | 6.32 | 0.40 | 6.38 | 0.40 | 6.33 | 0.37 | 6.33 |
| GVMi | 0.05 | 7.23 | 0.25 | 6.21 | 0.44 | 6.16 | 0.44 | 6.15 | 0.41 | 6.14 |

Table 8. Cont.

| Vegetation Indexes | Cumulative Leaf Number | | | | | | | | | |
|----------------------|------------------------|------|----------------|------|----------------|------|----------------|------|----------------|------|
| | Top 1 | | Top 2 | | Top 3 | | Top 4 | | Top 5 | |
| | R ² | RMSE | R ² | RMSE | R ² | RMSE | R ² | RMSE | R ² | RMSE |
| NDVI | 0.01 | 7.40 | 0.15 | 6.64 | 0.18 | 7.44 | 0.17 | 7.46 | 0.15 | 7.36 |
| NDMI | 0.00 | 7.42 | 0.00 | 7.17 | 0.13 | 7.68 | 0.13 | 7.62 | 0.13 | 7.45 |
| NDII/NDMI | 0.05 | 7.24 | 0.12 | 6.74 | 0.34 | 6.68 | 0.36 | 6.56 | 0.35 | 6.42 |
| NDII ₂₀₂₀ | 0.01 | 7.38 | 0.19 | 6.47 | 0.25 | 7.12 | 0.23 | 7.16 | 0.21 | 7.07 |
| MSI ₂₀₂₀ | 0.02 | 7.37 | 0.20 | 6.45 | 0.26 | 7.05 | 0.25 | 7.09 | 0.23 | 7.00 |

(d) EWT

| Vegetation Indexes | Cumulative Leaf Number | | | | | | | | | |
|------------------------|------------------------|--------|----------------|--------|----------------|--------|----------------|--------|----------------|--------|
| | Top 1 | | Top 2 | | Top 3 | | Top 4 | | Top 5 | |
| | R ² | RMSE | R ² | RMSE | R ² | RMSE | R ² | RMSE | R ² | RMSE |
| WI | 0.29 | 0.0025 | 0.14 | 0.0039 | 0.21 | 0.0048 | 0.24 | 0.0046 | 0.25 | 0.0046 |
| NDWI | 0.32 | 0.0024 | 0.24 | 0.0037 | 0.38 | 0.0042 | 0.43 | 0.0040 | 0.43 | 0.0040 |
| MSI | 0.30 | 0.0025 | 0.17 | 0.0039 | 0.28 | 0.0046 | 0.30 | 0.0044 | 0.31 | 0.0044 |
| NDII | 0.31 | 0.0025 | 0.18 | 0.0038 | 0.29 | 0.0045 | 0.32 | 0.0044 | 0.33 | 0.0043 |
| RMSI | 0.31 | 0.0025 | 0.18 | 0.0038 | 0.26 | 0.0046 | 0.30 | 0.0044 | 0.31 | 0.0044 |
| GVMi | 0.29 | 0.0025 | 0.11 | 0.0040 | 0.17 | 0.0049 | 0.20 | 0.0048 | 0.20 | 0.0047 |
| NDVI | 0.24 | 0.0026 | 0.39 | 0.0033 | 0.42 | 0.0040 | 0.43 | 0.0040 | 0.44 | 0.0040 |
| CI _{red edge} | 0.36 | 0.0024 | 0.33 | 0.0035 | 0.35 | 0.0044 | 0.37 | 0.0042 | 0.37 | 0.0042 |
| NDMI | 0.18 | 0.0027 | 0.15 | 0.0039 | 0.14 | 0.0050 | 0.16 | 0.0049 | 0.15 | 0.0049 |
| NDII/NDMI | 0.18 | 0.0027 | 0.02 | 0.0042 | 0.02 | 0.0053 | 0.02 | 0.0053 | 0.03 | 0.0052 |
| NDII ₂₀₂₀ | 0.29 | 0.0025 | 0.30 | 0.0035 | 0.48 | 0.0039 | 0.49 | 0.0038 | 0.49 | 0.0038 |
| MSI ₂₀₂₀ | 0.31 | 0.0025 | 0.32 | 0.0035 | 0.50 | 0.0038 | 0.51 | 0.0037 | 0.52 | 0.0037 |

Understanding the vertical extent of water-related properties will affect decisions based on this. For instance, GWC_D can be used to evaluate fire risk. However, for vegetation with complex vertical architecture, whether GWC_D estimated based on canopy reflectance represents only the top leaf layers or they can also represent intermediate and the bottom leaf layers will be unknown without analysis of the vertical distribution. If GWC_D for the studied vegetation failed to represent the bottom layers, the evaluation of fire risk may not be accurate since the bottom layers might have higher or lower GWC_D than the estimation due to different ages and light conditions from the top layer. In addition, since radiative transfer model is based on the assumption of homogeneous vertical profile of vegetation, a complete vertical picture will also improve studies of EWT estimation based on the radiative transfer model inversion.

5. Conclusions

In this study, we analyzed the vertical distribution of four water-related properties (GWC_D , GWC_F , RWC, and EWT) within a winter wheat canopy during heading and early ripening stages, and evaluated how ‘deep’ remote sensing VIs derived from canopy spectra can ‘penetrate’ the winter wheat canopy and provide estimations of water-related properties. Our results demonstrated that the vertical distribution of GWC_D , GWC_F , RWC, and EWT followed a near-bell-shaped curve with the highest values at the intermediate leaf position and the lowest value at the bottom leaf. The water-related properties for the

cumulative leaf number within the canopy suggested that GWC_D and GWC_F of the top three can represent GWC of the whole plant during the heading stage and the early ripening stage. RWC and EWT of the whole plant should be calculated based on the top four leaves or all leaves. At leaf level, the analysis demonstrated strong relationships between EWT and VIs for the top leaf layer, but for GWC_D , GWC_F , and RWC, the strongest relationships with VIs were found in the intermediate leaf layers. At canopy level, water absorption- and greenness-based VIs provided the most accurate estimation of GWC_D and GWC_F for the top three or four leaves. Water absorption-based VIs were able to estimate EWT of winter wheat for the top four leaves, but the suitable bands sensitive to water absorptions should be carefully selected for the studied species.

These observations indicated a theoretical basis of using remote sensing techniques to estimate canopy water-related properties, especially for imaging data. Spectral reflectance, measured above the canopy, may not be responsible for the incoming radiation interacting with bottom leaf layers of the plant, thus resulting in estimation errors of properties of the whole canopy. However, our hypothesis was that in wheat the cumulative properties of top three layers, which can be sensed by remote sensors, may well represent total canopy properties. Similar results of chlorophyll content showed that VIs based on red edge spectra can sense seven to nine leaf layers in maize, which is quite representative of the total chlorophyll content in the whole plant [33,49].

Nevertheless, to our knowledge, this is the first study to investigate the vertical distribution of water-related properties within a canopy and its impact on the estimation of water-related properties at leaf and canopy level with remote sensing VIs. Results of this study provided insights into remote estimation of vegetation water content and crop water stress monitoring. In future work, advanced spectroscopic analysis techniques (e.g., machine learning methods, genetic algorithms) can be incorporated to develop the indicators sensitive to water content in the whole canopy, and the impact of canopy vertical heterogeneity on biophysical and biochemical parameters of vegetation should be further analyzed for different species.

Acknowledgements

This work is supported by the Fundamental Research Funds for the Central Universities, China (grant number 2662013BQ020) and by State 863, China (grant number 2013AA102401).

Author Contributions

Shishi Liu provided the majority of the writing of this paper. Yi Peng contributed to a part of introduction and methods, and provided write ups in the discussion section. Wei Du, Yuan Le, and Lu Li took the measurements and processed data used in this paper.

Conflicts of Interest

The authors declare no conflicts of interest.

References

1. Zygielbaum, A.I.; Gitelson, A.A.; Arkebauer, T.J.; Rundquist, D.C. Non-destructive detection of water stress and estimation of relative water content in maize. *Geophys. Res. Lett.* **2009**, *36*, doi:10.1029/2009GL038906.
2. Rossini, M.; Fava, F.; Cogliati, S.; Meroni, M.; Marchesi, A.; Panigada, C.; Giardino, C.; Busetto, L.; Migliavacca, M.; Amaducci, S.; *et al.* Assessing canopy PRI from airborne imagery to map water stress in maize. *ISPRS J. Photogramm. Remote Sens.* **2013**, *86*, 168–177.
3. Thenkabail, P.S.; Gumma, M.K.; Teluguntla, P.; Mohammed, I.A. Hyperspectral remote sensing of vegetation and agricultural crops. *Photogramm. Eng. Remote Sens.* **2014**, *80*, 697–709.
4. Gao, B.C. NDWI, a normalized difference water index for remote sensing of vegetation liquid water from space. *Remote Sens. Environ.* **1996**, *58*, 257–266.
5. Zarco-Tejada, P.J.; Rueda, C.A.; Ustin, S.L. Water content estimation in vegetation with MODIS reflectance data and model inversion methods. *Remote Sens. Environ.* **2003**, *85*, 109–124.
6. Colombo, R.; Busetto, L.; Meroni, M.; Rossini, M.; Panigada, C. Optical remote sensing of vegetation water content. In *Hyperspectral Remote Sensing of Vegetation*; Thenkabail, P.S., Lyon, G.J., Huete, A., Eds., CRC Press, Taylor and Francis group: Boca Raton, FL, USA, 2012; pp. 227–238.
7. Sims, D.A.; Gamon, J.A. Estimation of vegetation water content and photosynthetic tissue area from spectral reflectance: A comparison of indices based on liquid water and chlorophyll absorption features. *Remote Sens. Environ.* **2003**, *84*, 526–537.
8. Datt, B. Remote sensing of water content in Eucalyptus leaves. *Aust. J. Bot.* **1999**, *47*, 909–923.
9. Colombo, R.; Meroni, M.; Marchesi, A.; Busetto, L.; Rossini, M.; Giardino, C.; Panigada, C. Estimation of leaf and canopy water content in poplar plantations by means of hyperspectral indices and inverse modeling. *Remote Sens. Environ.* **2008**, *112*, 1820–1834.
10. Yebra, M.; Dennison, P.E.; Chuvieco, E.; Riaño, D.; Zylstra, P.; Hunt, E.R.; Danson, F.M.; Qi, Y.; Jurdao, S.A. A global review of remote sensing of live fuel moisture content for fire danger assessment: Moving towards operational products. *Remote Sens. Environ.* **2013**, *136*, 455–468.
11. Hunt, E.R., Jr.; Rock, B.N. Detection of changes in leaf water content using near- and middle-infrared reflectances. *Remote Sens. Environ.* **1989**, *30*, 43–54.
12. Hunt, E.R., Jr. Airborne remote sensing of canopy water thickness scaled from leaf spectrometer data. *Int. J. Remote Sens.* **1991**, *12*, 643–649.
13. Peñuelas, J.; Piñol, J.; Ogaya, R.; Filella, I. Estimation of plant water concentration by the reflectance water index (R900/R970). *Int. J. Remote Sens.* **1997**, *18*, 2869–2875.
14. Hardisky, M.; Klemas, V.; Smart, R. The influence of soil salinity, growth form, and leaf moisture on the spectral radiance of *Spartina alterniflora* canopies. *Photogramm. Eng. Remote Sens.* **1983**, *49*, 77–83.
15. Ceccato, P.; Flasse, S.; Tarantola, S.; Jacquemoud, S.; Gregoire, J.M. Detecting vegetation leaf water content using reflectance in the optical domain. *Remote Sens. Environ.* **2001**, *77*, 22–33.
16. Dennison, P.E.; Roberts, D.A.; Thorgusen, S.R.; Regelbrugge, J.C.; Weise, D.; Lee, C. Modeling seasonal changes in live fuel moisture and equivalent water thickness using a cumulative water balance index. *Remote Sens. Environ.* **2003**, *88*, 442–452.

17. Wang, L.L.; Hunt, E.R.; Qu, J.J.; Hao, X.J.; Daughtry, C.S.T. Remote sensing of fuel moisture content from ratios of narrow-band vegetation water and dry-matter indices. *Remote Sens. Environ.* **2013**, *129*, 103–110.
18. Ustin, S.L.; Roberts, D.A.; Pinzón, J.; Jacquemoud, S.; Gardner, M.; Scheer, G.C.; Castañeda, C.M.; Palacios-Orueta, A. Estimating canopy water content of chaparral shrubs using optical methods. *Remote Sens. Environ.* **1998**, *65*, 280–291.
19. Ustin, S.L.; Riano, D.; Hunt, E.R. Estimating canopy water content from spectroscopy. *Isr. J. Plant Sci.* **2012**, *60*, 9–23.
20. Casas, A.; Riaño, D.; Ustin, S.L.; Dennison, P.; Salas, J. Estimation of water-related biochemical and biophysical vegetation properties using multitemporal airborne hyperspectral data and its comparison to MODIS spectral response. *Remote Sens. Environ.* **2014**, *148*, 28–41.
21. Stow, D.; Niphadkar, M.; Kaiser, J. MODIS-derived visible atmospherically resistant index for monitoring chaparral moisture content. *Int. J. Remote Sens.* **2005**, *26*, 3867–3873.
22. Yebra, M.; Chuvieco, E.; Riano, D. Estimation of live fuel moisture content from MODIS images for fire risk assessment. *Agric. For. Meteorol.* **2008**, *148*, 523–536.
23. Riaño, D.; Vaughan, P.; Chuvieco, E.; Zarco-Tejada, P.J.; Ustin, S.L. Estimation of fuel moisture content by inversion of radiative transfer models to simulate equivalent water thickness and dry matter content: Analysis at leaf and canopy level. *IEEE Trans. Geosci. Remote Sens.* **2005**, *43*, 819–826.
24. Dawson, T.P.; Curran, P.J.; Plummer, S.E. The biochemical decomposition of slash pine needles from reflectance spectra using neural networks. *Int. J. Remote Sens.* **1998**, *19*, 1433–1438.
25. Cheng, T.; Rivard, B.; Sánchez-Azofeifa, A. Spectroscopic determination of leaf water content using continuous wavelet analysis. *Remote Sens. Environ.* **2011**, *115*, 659–670.
26. Li, L.; Ustin, S.L.; Riaño, D. Retrieval of fresh leaf fuel moisture content using Genetic Algorithm Partial Least Squares (GA-PLS) modeling. *IEEE Geosci. Remote Sens. Lett.* **2007**, *4*, 216–220.
27. Qi, Y.; Dennison, P.E.; Matt Jolly, W.; Kropp, R.C.; Brewer, S.C. Spectroscopic analysis of seasonal changes in live fuel moisture content and leaf dry mass. *Remote Sens. Environ.* **2014**, *150*, 198–206.
28. Anderson, M.C. Stand structure and light penetration. 2. A theoretical analysis. *J. Appl. Ecol.* **1966**, *3*, 41–54.
29. Tucker, C.J. Asymptotic nature of grass canopy spectral reflectance. *Appl. Opt.* **1977**, *16*, 1151–1156.
30. Koetz, B.; Baret, F.; Polive, H.; Hill, J. Use of coupled canopy structure dynamic and radiative transfer models to estimate biophysical canopy characteristics. *Remote Sens. Environ.* **2005**, *95*, 115–124.
31. Darvishzadeh, R.; Skidmore, A.; Schlerf, M.; Atzberger, C. Inversion of a radiative transfer model for estimating vegetation LAI and chlorophyll in a heterogeneous grassland. *Remote Sens. Environ.* **2008**, *112*, 2592–2604.
32. Keating, B.A.; Wafula, B.M. Modelling the fully expanded area of maize leaves. *Field Crops Res.* **1992**, *29*, 163–176.
33. Ciganda, V.; Gitelson, A.A.; Schepers, J. Vertical profile and temporal variation of chlorophyll in maize canopy: Quantitative “crop vigor” indicator by means of reflectance-based techniques. *Agron. J.* **2008**, *100*, 1409–1417.

34. Winterhalter, L.; Mistele, B.; Schmidhalter, U. Assessing the vertical footprint of reflectance measurements to characterize nitrogen uptake and biomass distribution in maize canopies. *Field Crops Res.* **2012**, *129*, 14–20.
35. Valentinuz, O.R.; Tollenaar, M. Vertical profile of leaf senescence during the grain-filling period in older and newer maize hybrids. *Crop. Sci.* **2004**, *44*, 827–834.
36. Ceccato, P.; Gobron, N.; Flasse, S.; Pinty, B.; Tarantola, S. Designing a spectral index to estimate vegetation water content from remote sensing data: Part 1 Theoretical approach. *Remote Sens. Environ.* **2002**, *82*, 188–197.
37. Ceccato, P.; Flasse, S.; Gregoire, J.M. Designing a spectral index to estimate vegetation water content from remote sensing data: Part 2 Validation and applications. *Remote Sens. Environ.* **2002**, *82*, 198–207.
38. Tucker, C.J. Red and photographic infrared linear combinations for monitoring vegetation. *Remote Sens. Environ.* **1979**, *8*, 127–150.
39. Wang, L.; Hunt, J.E. R.; Qu, J.J.; Hao, X.; Daughtry, C.S.T. Towards estimation of canopy foliar biomass with spectral reflectance measurements. *Remote Sens. Environ.* **2011**, *115*, 836–840.
40. Wang, Q.; Li, P. Identification of robust hyperspectral indices on forest leaf water content using PROSPECT simulated dataset and field reflectance measurements. *Hydrol. Process.* **2012**, *26*, 1230–1241.
41. Gitelson, A.A.; Viña, A.; Rundquist, D.C.; Ciganda, V.; Arkebauer, T.J. Remote estimation of canopy chlorophyll content in crops. *Geophys. Res. Lett.* **2005**, *32*, doi:10.1029/2005GL022688.
42. Danson, F.M.; Bowyer, P. Estimating live fuel moisture content from remotely sensed reflectance. *Remote Sens. Environ.* **2004**, *92*, 309–321.
43. Maki, M.; Ishihara, M.; Tamura, M. Estimation of leaf water status to monitor the risk of forest fires by using remotely sensed data. *Remote Sens. Environ.* **2004**, *90*, 441–450.
44. Bowman, W.D. The relationship between leaf water status, gas exchange, and spectral reflectance in cotton leaves. *Remote Sens. Environ.* **1989**, *30*, 249–255.
45. Pierce, L.L.; Running, S.W.; Riggs, G.A. Remote detection of canopy water stress in coniferous forests using the NS001 thematic mapper simulator and the thermal infrared multispectral scanner. *Photogramm. Eng. Remote Sens.* **1990**, *56*, 579–586.
46. Cohen, W.B. Temporal versus spatial variation in leaf reflectance under changing water-stress conditions. *Int. J. Remote Sens.* **1991**, *12*, 1865–1876.
47. Riggs, G.A.; Running, S.W. Detection of canopy water stress in conifers using the airborne imaging spectrometer. *Remote Sens. Environ.* **1991**, *35*, 51–68.
48. Broge, N.H.; Mortensen, J.V. Deriving green crop area index and canopy chlorophyll density of winter wheat from spectral reflectance data. *Remote Sens. Environ.* **2002**, *81*, 45–57.
49. Ciganda, V.; Gitelson, A.A.; Schepers, J. Non-destructive determination of maize leaf and canopy chlorophyll content. *J. Plant. Physiol.* **2009**, *166*, 157–167.